

Opposed Flow Flame Spread Over Thin Solid Fuels: A 2D Numerical Study on Flame-Spread Transition from Normal Gravity to Zero Gravity and Vice Versa

Chenthil Kumar^a and Amit Kumar^a

^aDepartment of Aerospace Engineering, IIT Madras, Chennai, India

Abstract

An unsteady two dimensional numerical model of flame spread is formulated to study the transient flame spread over thin solid fuels. The work focuses on the study of transient flame spread from a steady normal gravity flame to micro gravity flame and vice versa. The gas-phase is described by two-dimensional governing equations comprising of full Navier-Stokes equations for laminar flow along with the conservation equations of mass, energy and species. The specie equations are for fuel vapor, oxygen, carbon dioxide and water vapor. A one-step, second-order finite rate Arrhenius reaction between fuel vapor and oxygen is assumed. The thin solid fuel model comprises of equations of continuity and energy in the one-dimension parallel to the solid fuel surface along with a solid fuel pyrolysis law. The solid fuel considered here is an aerodynamically and thermally thin cellulosic material. The solid is assumed to burn ideally *i.e.* it vaporizes to form fuel vapors without melting. The radiation transport is modeled by two-dimensional Radiative Transfer Equation, which is solved using Discrete Ordinates Method. The system of coupled partial differential equations for the flow and combustion in the gas phase is solved numerically using SIMPLER algorithm with a single step multi-grid technique for faster convergence. In normal gravity to zero-gravity transition the flame spread rate peaks ($V_f = 5.96$ cm/s) above steady state spread rate at zero gravity(5.32cm/s) at about 1.5 second and then decreases slowly to the steady state value (with in 5%) at about 3 seconds. Thus the experiments conducted in short duration (2s or less) drop tower may not reach steady state in the time available. On the other hand in 0g-1g transition steady state reached by about 1s. In both cases flame spread transient was oscillatory due to different response time of gas and solid phases. This was reflected in the phase behavior that the instantaneous spread rate and the integrated net heat flux in the preheat region were not in phase.

1. INTRODUCTION

Flame spread over solids is a classic combustion problem studied extensively to understand combustion process involving gas phase interaction with a solid phase fuel source. The interest in this class of problems is specifically driven by the need to have better fire safety with proper understanding of flame spread phenomena. Researchers have studied this problem for over five decades now, which has resulted in significant contribution to the understanding of the flame spread phenomena. Yet, because of the inherently complex nature of the problem due to its multi-dimensional characteristics and non linear inter-coupling of the transport process of flow, heat and mass transfer, many aspects remain elusive. One area of interest in the recent years has been the flame spread phenomena in microgravity environment. For most practical purposes microgravity experience is far less compared to terrestrial experience. And limited experiments and numerical work has shown that flames behave very differently and even counter intuitive in microgravity environment. Therefore a systematic study is needed to understand heat and mass transfer processes controlling spread phenomena in microgravity

environment. The recent human endeavor in space has necessitated better fire safety. The approach of almost all research has been to study a simplified configuration where dimensionality is reduced, and the external flow is simplified (parallel to the surface). Traditionally the flame spread phenomena is studied under two broad classifications namely: opposed flow flame spread and concurrent flow flame spread. This classification is based on the relative direction of flame spread with respect to the ambient velocity vector. In opposed flow spread the flame spread against the flow direction and in concurrent flow spread the flame spreads in the direction of flow. A special case of opposed flow spread is downward flame spread where the flame spreads vertically downward against gravity. In this work flame spread phenomena is studied in the opposed flow configuration.

The previous studies on unsteady flame spread over thin solid fuel were focused on the ignition and subsequent transient to steady flame spread [1-3], extinction of flames [4] and transition of concurrent to opposed flow flame spread in micro-gravity [5]. The microgravity combustion experiments are most economically conducted on earth in drop towers or aboard aircraft following parabolic flight path trajectory. While in drop towers the available time is usually small (1s to a maximum of about 10s), flight based experiments are subjected to g-jitters due to atmospheric/aerodynamic disturbances. Therefore quite a significant part of earth based experiments could exhibit unsteady behavior. So far, the flame spread transient with gravity has not been studied. This serves the motivation to the present study.

Present work focus on one such application of sudden transition from normal gravity to microgravity (here equivalently zero gravity) environment which is experienced in drop towers. For the particular study, the existing steady opposed flow flame spread 2D model was modified for the unsteady state to study the transient spread.

2. NUMERICAL MODEL AND NUMERICAL SCHEME

The numerical model consists of unsteady governing equations in gas and solid phases formulated for the opposed-flow spread in the flame-fixed coordinate system. Since the flame spread rate can change with time, the governing equations are written in non-inertial frame of reference. The assumptions made in modeling opposed flow flame spread over thin solids is listed below.

1. The solid is assumed to be thin (both thermally and aerodynamically). For a thermally thin fuel the temperature is constant across its thickness. Yet another implication of thermally thin assumption is that conduction along the length and across the width of solid be neglected on account of smaller characteristic conduction distance through the fuel compared with that in the gas phase. The aerodynamically thin condition implies that the flame standoff distance is much greater than the thickness of the solid so that the solid phase boundary conditions are applied at $Y = 0$.
2. As the flame spreads, the finite length of fresh fuel ahead of flame decreases in time. In present formulation flame spread is considered for fixed fuel length ahead of flame. This flame is assumed to represent the instantaneous flame in the inherently unsteady spread. This assumption holds if entrance length ahead of flame of gas is larger compared to the thermal length scale.
3. The solid is assumed to burn ideally *i.e.* it vaporizes to form fuel vapors without melting or forming ash.
4. The solid radiation is assumed to be diffuse.
5. The flow velocities in this work are small ($< 1-2\text{m/s}$) so the flow is assumed to be laminar.

2.1 Gas Phase Model

The gas phase model consists of two-dimensional Navier-Stokes equations for laminar flow along with the conservation equations of mass, energy and species. The species equations are for fuel vapor, oxygen, carbon dioxide and water vapor. The governing equations are presented in non-dimensional form. The normalization procedure is similar to the one used by reference [6-8]. A one-step, second-order, finite rate Arrhenius reaction between fuel vapor and oxygen is assumed. The governing equations are presented in a non-dimensional form. In these equations, V_p, X_e , the reference properties (with * superscript) and the variables with overhead bar indicate dimensional quantities. The rest are non-dimensional quantities. The length scale chosen for normalization is the thermal length, $L_R = \alpha^* / \bar{U}_R$, (where α^* is thermal diffusivity of gas) which is obtained by considering the balance of convection and conduction in the gas phase flame

stabilization zone. The reference velocity \bar{U}_R (defined later) is used to normalize velocity and the ambient temperature, \bar{T}_∞ is used to normalize temperature. The gas phase time scale chosen is $T_R = (L_R^* L_R) / \alpha^*$. Pressure is normalized by the ambient value of 1atm (\bar{P}_∞) and is normalized as $P = (\bar{P} - \bar{P}_\infty) / \rho^* \bar{U}_R^2$. All thermal and transport properties are normalized by their values at the reference temperature, T^* (1250 K), which is the average of the adiabatic flame temperature in air and the ambient temperature. Specific heats are a function of temperature for each species and are obtained from standard references. The transport properties are modeled following Smooke and Giovangigli [9], as

$$\mu = T^{0.7}, \quad \kappa / c_p = T^{0.7}, \quad \rho D_i = T^{0.7},$$

where

$$i = F, O_2, CO_2, H_2O, N_2$$

Specific heat depends on the composition of the mixture and the temperature. Specific heat for each species in polynomial form were taken from reference[10, 11]

The non-inertial term is added to predict the non-inertial behavior of the flame with respect to the flame fixed location along the x-direction. The non-dimensional governing equations and the boundary conditions in the gas phase are summarized below.

Continuity equation

$$\frac{\partial \rho}{\partial t} + \nabla \cdot (\rho \vec{U}) = 0 \tag{1}$$

X-Momentum Equation

$$\begin{aligned} \frac{\partial(\rho u)}{\partial t} + \nabla \cdot \left[\rho u \vec{U} - \left(\frac{\mu}{\text{Re}} \right) \nabla u \right] &= -p_x + \left(\frac{1}{\text{Re}} \right) \\ \left\{ \left[\frac{1}{3} \mu u_x - \frac{2}{3} \mu (v_y) \right]_x + [\mu v_x]_y \right\} &+ \left(\frac{U_B}{U_R} \right)^3 \frac{(\rho - \rho_\infty)}{(\rho_f - \rho_\infty)} g \\ - \left(\frac{dV_f}{dt} \right) \frac{(\rho - \rho_\infty)}{(\rho_f - \rho_\infty)} & \end{aligned} \tag{2}$$

Y-Momentum Equation

$$\begin{aligned} \frac{\partial(\rho v)}{\partial t} + \nabla \cdot \left[\rho v \vec{U} - \left(\frac{\mu}{\text{Re}} \right) \nabla v \right] &= -p_y + \left(\frac{1}{\text{Re}} \right) \\ \left\{ [\mu u_y]_x + \left[\frac{1}{3} \mu v_y - \frac{2}{3} \mu (u_x) \right]_y \right\} & \\ \text{Re} = \frac{\bar{L}_R \bar{U}_R \rho^*}{\mu^*}, \quad L_R = \frac{\alpha^*}{\bar{U}_R} \quad T_R = \frac{(L_R^* L_R)}{\alpha^*} & \quad \bar{U}_R = \bar{U}_\infty + \bar{U}_B + V_f \end{aligned} \tag{3}$$

where

$\bar{U}_B = [g_R \beta_R (T_\infty - T_F) \alpha^*]^{1/3}$ is the reference buoyancy induced velocity and \bar{U}_∞ is the imposed forced velocity at the inlet.

Specie equation

$$\frac{\partial(\rho Y_i)}{\partial t} + \nabla \cdot \left[\rho Y_i \vec{U} - \left(\frac{1}{Le_i} \right) (\rho D_i \nabla Y_i) \right] = \dot{\omega}_i''' \tag{4}$$

where $i = F, O_2, CO_2, H_2O, N_2$

$$Le_i = \frac{\text{diffusion time}}{\text{convection or conduction time}},$$

$$= \frac{\bar{L}_R^2 / D_i^*}{\bar{L}_R / \bar{U}_R} = \frac{\bar{L}_R^2 / D_i^*}{\bar{L}_R / \alpha^*} = \frac{\alpha^*}{D_i^*}$$

Lewis number for species i

$$Le_{F_i} = 1.0 \quad Le_{O_2} = 1.11 \quad Le_{CO_2} = 1.39 \quad Le_{H_2O} = 0.83 \quad Le_{N_2} = 1.0$$

$$\dot{\omega}_i^m = f_i \dot{\omega}_F^m = f_i Da \rho^2 Y_F Y_{O_2} \exp\left(-\frac{E_g}{T}\right)$$

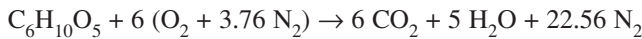
$$\text{where } Da = \frac{\text{characteristic flow time}}{\text{characteristic reaction time}} = \frac{\bar{L}_R / \bar{U}_R}{\rho^* / \rho^{*2} \bar{B}_g} = \frac{\bar{B}_g \rho^* \bar{L}_R}{\bar{U}_R} = \frac{\bar{B}_g \rho^* \alpha^*}{\bar{U}_R^2}$$

f_i = stoichiometric mass ratio of species i and fuel

E_g = non-dimensional gas phase activation energy (50.3)

\bar{B}_g = gas phase pre-exponential factor ($1.58 \times 10^9 \text{ m}^3/\text{Kg/s}$)

The fuel is cellulose with the formula $C_6H_{10}O_5$. The stoichiometric combustion of fuel in air can thus be written as:



For the above one-step cellulose and air stoichiometric reaction, the stoichiometric ratios are, $f_F = -1$, $f_{O_2} = -1.1852$, $f_{CO_2} = 1.6296$, $f_{H_2O} = 0.5556$, $f_{N_2} = 3.901$

Energy Equation

$$\frac{\partial(\rho c_p T)}{\partial t} + c_p \nabla \cdot \left[\rho T \bar{U} - \left(\frac{\kappa}{c_p} \nabla T \right) \right] =$$

$$\sum_{i=1}^N \left(\frac{1}{Le_i} \right) \rho D_i c_{p,i} (\nabla Y_i \cdot \nabla T) -$$

$$\sum_{i=1}^N \dot{\omega}_i^m h_i + \nabla c_p \cdot \nabla T \left(\frac{\kappa}{c_p} \right) - \left(\frac{1}{B_0} \right) \nabla \cdot \vec{q}_r \quad (5)$$

$$\text{where } c_p = \sum_{i=1}^N c_{p,i} Y_i, \quad h_i = \frac{(\bar{h}_i^0 + \int_{\bar{T}_0=298K}^{\bar{T}} \bar{c}_{p,i} d\bar{T})}{(c_p^* \bar{T}_\infty)}$$

$Bo = \rho^* c_p^* U_R l / (\sigma T_\infty^3)$ The term $\nabla \cdot \vec{q}_r$ accounts for energy exchange due to radiative participating media.

Radiation treatment

A direct treatment of radiation involves solving the Radiative Transfer Equation (RTE) for intensity distribution over the domain of interest. Since solving the Radiative Transfer Equation with spectral accuracy is computationally prohibitive for this coupled multi-dimensional problem, the use of mean absorption coefficients is adopted. The transfer equation for radiation energy in non-dimensional form passing in a specified direction $\vec{\Omega}$ through a small differential volume in an emitting, absorbing and non-scattering gray medium, in the two dimensional co-ordinates can be written as

$$\xi \frac{\partial I(x, y, \Omega)}{\partial x} + \eta \frac{\partial I(x, y, \Omega)}{\partial y} + \beta(x, y) I(x, y, \Omega) = \alpha(x, y) I_b(x, y) + \frac{\sigma}{4\pi} \int_{\Omega_i=4\pi} I(x, y, \Omega_i) d\Omega_i \quad (6)$$

ξ, η = direction cosines in x and y direction.

In this work, the participating gases are carbon dioxide and water vapor. Soot is assumed to be absent based on the experiment observation on flame in low-speed flow in low oxygen atmosphere [12]. The simplest way is to assign a constant absorption coefficient, which is treated as a parameter in [13]. A more sophisticated treatment of gas radiation has been proposed in [14]. In work by Lin and Chen [15], with an optically thin limit approximation, variable absorption coefficients based on local mixture composition and temperature were used and two-dimensional Radiative transfer equations was solved using P-1 approximation. In concurrent flame spread, Jiang [7] solved the radiation transfer equation using discrete ordinate method but again an optical-thin flame is assumed with the adaptation local Planck-mean absorption coefficient. Here a mean absorption coefficient $K(x, y)$ for the gas mixture is calculated by the local Planck-mean absorption coefficient.

$$K_p = P_{CO_2} \cdot K_{p(CO_2)} + P_{H_2O} \cdot K_{p(H_2O)}, K(x, y) = C * K_p$$

The correction factor C has taken from reference [16]. The solid fuel is assumed to be diffusively emitting, transmitting and reflecting. Because of the symmetry of the flame with respect to solid, the transmitted radiation is equivalent to the reflected radiation. So the solid total absorptance α alone is sufficient to characterize the response of the solid surface to the incident radiation. The only other quantity needed to complete the description of solid radiation is the solid total emittance ε . Note that the solid can be radiatively spectral, because incident gas radiation comes from high temperature medium while surface emission is from lower temperature, the solid total absorptance α and the solid total emittance ε do not have to be equal Pettegrew et al. [17]. The outgoing radiative intensity from the wall $y = y_{\min} = 0$ can be expressed as

$$I(r_w, \Omega) = \varepsilon(r_w) I_b(r_w) + \frac{(1-\alpha)}{\pi} \int_{n\Omega < 0} |n \cdot \Omega| I(r_w, \Omega') d\Omega' \quad (7)$$

where $n\Omega > 0$. Once the radiative intensity field is obtained, the total incident radiation, radiative flux, and the divergence of radiative flux in the rectangular domain is obtained from the following formula:

$$\text{Incident radiation: } G(x, y) = \int_{4\pi} I(x, y, \Omega) d\Omega$$

The divergence of radiative flux for the assumptions of emitting, absorbing and non-scattering gray is given below.

$$\nabla \cdot q_r(x, y) = \alpha(x, y) [4\sigma T^4(x, y) - G(x, y)] \quad (8)$$

Boundary conditions

The boundary conditions in the gas phase are presented below.

At $X = x_{\max}$ (upstream or inlet)

$$u = (\bar{U}_\infty - V_f) / \bar{U}_R, v = 0$$

$$T = 1$$

$$Y_{O_2} = Y_{O_2, \text{inlet}}, Y_i = 0 \quad (i = F, CO_2, H_2O)$$

At $X = x_{\min}$ (downstream or exit)

$$u_x = 0, v_x = 0,$$

if $u > 0$, $T = 1$, $Y_{O_2} = Y_{O_2,\infty}$, $Y_i = 0$,

where $i = CO_2, H_2O, F$

if $u \leq 0$, $T_x = 0$, $(Y_i)_x = 0$

where $i = O_2, CO_2, H_2O, F$

At $Y = 0$ (Fuel surface or Y symmetry plane)

$$u = -V_f / \bar{U}_R, v = v_w, T = T_s \quad \dot{m}Y_{F,w} = \dot{m} + \frac{\rho D_F}{Le_F} \left(\frac{\partial Y_F}{\partial y} \right)_w,$$

$$\dot{m}Y_{i,w} = \frac{\rho D_i}{Le_i} \left(\frac{\partial Y_i}{\partial y} \right)_w \quad (i = O_2, CO_2, H_2O)$$

Here the fuel vapor mass flux \dot{m} , blowing velocity v_w , and surface temperature T_s as functions of x and z are determined by the coupled solutions of the solid phase equations

For regions of complete fuel burnout (no insert)

$$u_y = 0, v = 0, T_y = 0, (Y_i)_y = 0$$

At $Y = y_{\max}$ at tunnel wall

$$u = -V_f / \bar{U}_R, v = 0, w = 0$$

$$T = 1, (Y_i)_y = 0 \quad (i = F, O_2, CO_2, H_2O)$$

2.2 Solid Phase Model

The unsteady thin solid fuel model comprises of equations of continuity and energy in one-dimensions along with a solid fuel pyrolysis law. The solid considered here is a cellulosic material with half thickness $\tau = 0.038\text{mm}$. The solid is assumed to burn ideally *i.e.*, it vaporizes to form fuel vapors without melting. The pyrolysis of fuel is modeled using a one-step, zeroth-order, Arrhenius kinetics and the radiation loss from the solid is included. The pyrolysis model relating fuel vapor mass flux from the solid to the surface temperature can be represented as

$$\dot{m} = A_s \rho_s \exp\left(\frac{-E_s}{T_s}\right) = \rho v_w \quad (9)$$

The solid density (ρ_s) is taken as a constant, while the thickness of the fuel (h) is assumed to change with pyrolysis. The blowing velocity distribution (v_w) along the fuel surface is determined from the fuel vapor mass flux and the gas phase density at the surface. In the flame fixed coordinates, the fuel feeds into the domain at a speed V_f where, V_f is the flame-spread rate and is an eigen value of this problem. The solid has two time scales; one is along fuel $T_{s1} = (\alpha_s) / (\bar{U}_R * \bar{U}_R)$ and the other across the fuel thickness h_s $T_{s2} = (h_s * h_s) / (\alpha_s)$. The governing equations for the fuel for steady spread are as follows.

Mass conservation:

$$\rho_s V_f (h)_x - \dot{m} = \left(\frac{\alpha^*}{\alpha_s} \right) \rho_s \frac{\partial h}{\partial t} \quad (10)$$

Combining the pyrolysis relation with the mass conservation, a relation between fuel thickness and surface temperature is obtained as

$$(h)_x = \frac{A_s}{V_f} \exp\left(\frac{-E_s}{T_s}\right) + \left(\frac{\alpha^*}{\alpha_s}\right) \frac{1}{V_f} \frac{\partial h}{\partial t}$$

Energy Equation:

$$\begin{aligned} q_c + \frac{q_r^y}{Bo} + \Gamma(hT_s)_x - \Gamma(h)_x [(1-c)T_L + (-L) + cT_s] \\ = \rho_s c_s \left(\frac{\alpha^*}{\alpha_s}\right) \frac{\partial(T_s h)}{\partial t} \end{aligned} \tag{11}$$

where

$$\Gamma = \frac{\bar{\rho}_s \bar{c}_s V_f}{\rho^* c_p^* \bar{U}_R}$$

On the left-hand side of the energy equation, the first term is the conductive heat flux from the gas phase (q_c). In the solid phase energy equation the terms describing the conduction through the solid fuel have been neglected based on thermally thin assumption discussed earlier. The second term is the radiation term due to solid phase radiation loss and $q_y = q^{y+} + q^{y-}$. The third term of the left-hand side represents bulk heat up term and the fourth left-hand side represents the energy change due to the latent heat of vaporization of the fuel. The right hand side represents the heat fluxes variation with time. The latent heat of the fuel (L) is specified at $\bar{T}_L = 300$ K. The boundary conditions for the solid phase governing equations are the prescribed fuel thickness and the surface temperature at fuel leading edge upstream of flame at

$$(x=x_0) \text{ i.e at } x = x_0 \begin{pmatrix} \text{leading edge of fuel} \\ \text{sample upstream of flame} \end{pmatrix}$$

$$T_s = 1, \quad h = \bar{\tau} / \bar{L}_R$$

The above set of governing equations and boundary conditions completely define the problem and are solved numerically.

2.3 Numerical Scheme

The system of coupled partial differential equations for the flow and combustion in the gas phase is solved numerically by SIMPLER algorithm [18]. The nonlinear equation sets are discretized using a finite-volume based difference technique. The velocities are stored at staggered grid locations with respect to the scalar variables. The resulting set of algebraic equations is solved by sweeping plane-by-plane in each direction. Along each plane, the line-by-line procedure is used, which is a combination of Gauss-Seidel and the tridiagonal matrix algorithm (TDMA). In addition, the gas-phase system is coupled to the solid-phase equations, which are solved by finite-difference technique. The flame spread rate (the eigenvalue of the whole system) is determined iteratively using the bisection method to force and the pyrolysis front (95% of the fresh fuel thickness) to occur at $X = 0$.

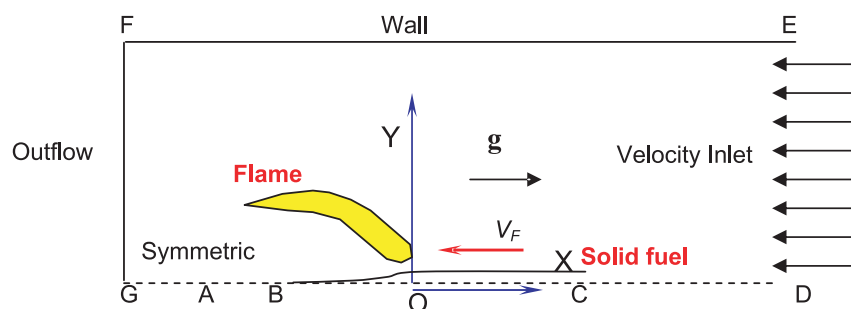


Figure 1. Schematic of problem domain

Figure 1 shows the schematic of the problem domain. The boundary DE is velocity inlet, FE is the wall, FG is outflow and GD is symmetry plane. In symmetry planes GA and CD are gradient free boundaries (no fuel), AC is the fuel surface along which B is the burnout location beyond which (i.e. section AB) only inert component is present. The gravity vector is in the direction opposite to the inlet velocity. The characteristic length scale in $1g$ & $0g$ environments are quite different. The small length scale characterizes small normal gravity flame which is located near to the solid fuel surface and a larger length scale characterizes zero-gravity flame which is long and located further from fuel surface. Hence to be consistent in computations the extent of computational domain is prescribed non-dimensionally (500 in Y direction and GA = 400 and CD = 200 in X direction) identically for both $1g$ & $0g$ cases. But since the fuel has specified physical length (AC = 100cm), the non-dimensional length (AC) will be different in $1g$ & $0g$ cases. Figure 1A and 1B shows the *dimensional* grid structure for the steady zero gravity and steady normal gravity flow problem.

The grid node distribution is non-uniform to account for the presence of one-dimensional fuel sample. Along Y direction the grid nodes are clustered at the fuel surface ($Y = 0$) to capture the flame structure and the transport processes with adequate accuracy. The smallest grid size at this location is 0.001 thermal length (characteristic length scale). The grid expands away from the fuel surface up to some intermediate distance and then contract to give clustered grid at upper wall. The grid node distribution along X is more complex due to the presence of finite size fuel specimen. The grid nodes are clustered around $X = 0$, which is the pyrolysis zone on column axis and also the flame-anchoring region. Here also the minimum grid size is 0.001 thermal lengths to accurately resolve large variations in the region.

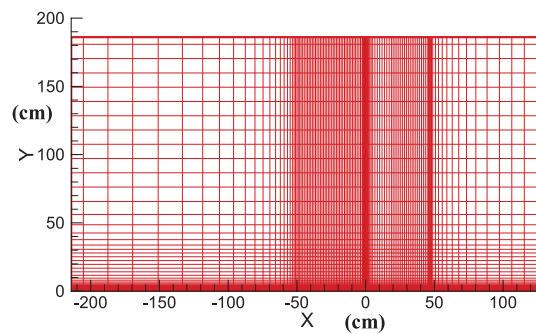


Figure 1A. Grid structure for zero-gravity flame spread simulation

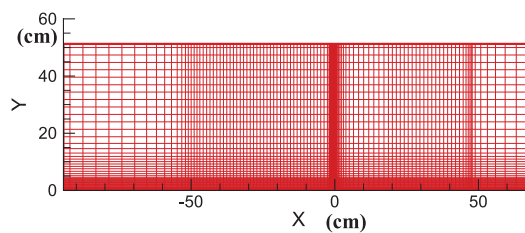


Figure 1B. Grid structure for normal gravity flame spread simulation

The grid node spacing expand away from $X = 0$ both in the upstream and the downstream directions. Fine grid structure in the burnout region is used to resolve the burnout location. Although it is difficult to ensure equally fine cells across the fuel width at all the pyrolysis fronts and burnout locations, in general grids are fine in the region. Grid nodes also cluster at the leading and the trailing edge of the fuel sample.

Both transient cases were computed on non dimensional grids. For transient studies (say $1g-0g$ transition) the steady state results for initial condition (i.e. $1g$) were interpolated on grid for the final state (i.e. $0g$). The interpolation was carried on physical scale to preserve the flame shape and structure.

3. RESULTS AND DISCUSSION

The numerical code for two-dimensional steady state model was validated against spread rate data from reference [19] for both normal gravity and zero-gravity flames at various oxygen concentrations. The normal gravity flame spread rate predictions at various oxygen concentration levels were close (maximum deviation is about 10%) to the experimental values. However, the zero-gravity simulations predicted higher flame spread rate (10-30%, higher for higher oxygen concentrations) than the experiments. This deviation from experimental values may be attributed to the three-dimensional effect of gas radiation which is a major heat transport mechanism in zero-gravity. In two dimensions the radiation heat loss remains under predicted and hence higher heat feed back to the solid fuel which results in over prediction of flame spread rates. Our on-going work on three-dimensional flame spread has confirmed the above reason.

In this study an unsteady extension of the two-dimensional steady state numerical code was used to carry out computation for a sudden change in gravity level from $1g$ to $0g$ which occurs in the beginning of a drop tower test. For comparison $0g$ to $1g$ sudden transition was also computed. The ambient oxygen in all the computations was taken to be 50% and the ambience was considered quiescent. The computed steady state spread rate at the normal gravity environment was 3.74cm/sec and that in zero gravity environment was 5.32cm/sec . The typical gas response time scale ($t_{gas,R} = \alpha^* / \bar{U}_R^2$) for the normal gravity and the zero gravity flames are 0.004s and 0.08s respectively. The typical solid phase time scale ($t_{solid,R} = \alpha^* / \bar{U}_R V_f$), for the normal gravity and zero gravity environment are 0.024s and 0.08s respectively. Therefore an overall time step of 0.001s was chosen for this computation study.

The computed results are presented in two sections. The first section describes flame spread transient for sudden transition from $1g$ to $0g$ environment and the second section describes the flame spread transient for sudden transition from $0g$ to $1g$ environment.

3.1 Flame spread transition from $1g$ to $0g$

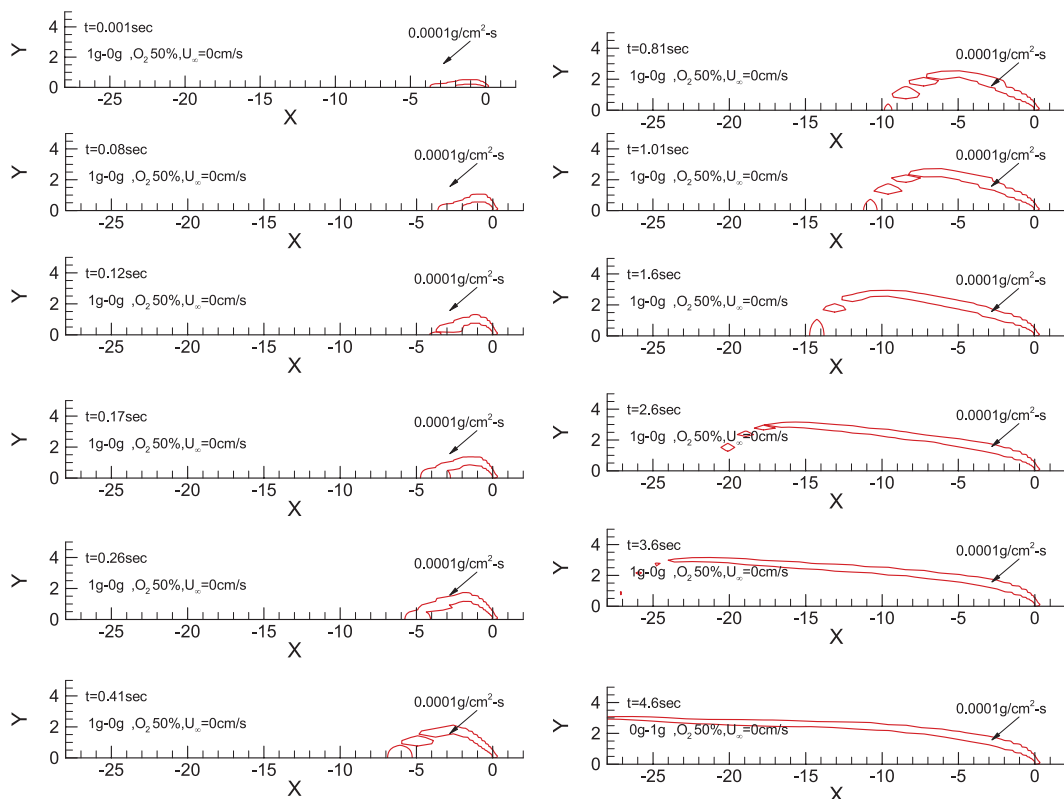


Figure 2. Flame shape (represented by reaction rate contour) at different instances of times for sudden transition from $1g$ to $0g$

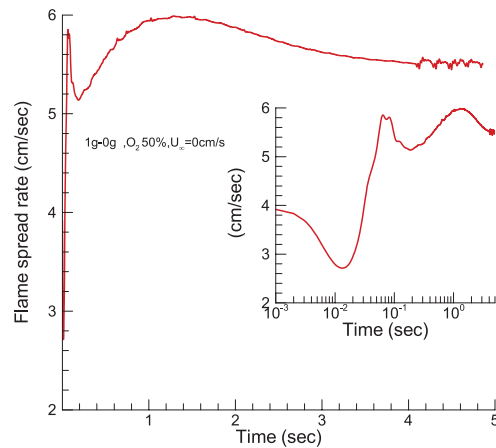


Figure 3. Flame spread rate variation with time for sudden transition from $1g$ to $0g$ environment

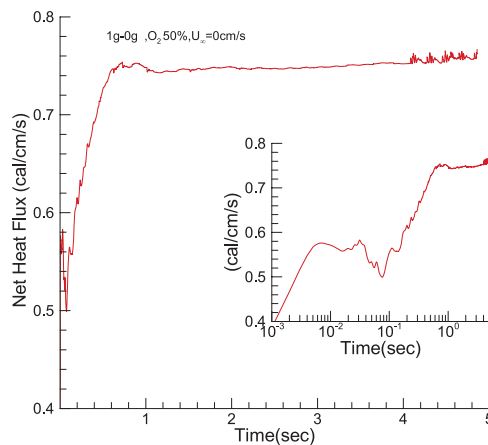


Figure 4. Variation of integrated net heat flux along preheated region with time for sudden transition from $1g$ to $0g$ environment

In a typical drop tower experiment, a steady state normal gravity flame spread is established prior to $t = 0$, at which the experiment capsule is dropped free creating a zero-gravity environment instantaneously. This situation is identically simulated here. Figure 2 shows transient flame snapshots at various times as flame evolves from normal gravity to zero-gravity flame. The visible flame is represented by the reaction rate contour for $10^{-4} \text{ g/cm}^3/\text{s}$ [4]. The normal gravity flame (flame shape close to one at $t = 0.001\text{s}$) is small and pushed close to surface by air entrained by the rising buoyant plume. Sudden removal of buoyant flow in absence of gravity the flame is seen to move away progressively from the surface. The response of the solid phase is reflected in the flame spread rate which peaks to $V_f = 5.96 \text{ cm/s}$ at about 1.5s after the drop and then decreases slowly to the steady state value for zero-gravity, within 5% at about 3s and exact value at about 4s. This suggests that experiments for the case conducted in short duration (say 2s or less) drop tower may not reach steady state in the time available. The experimental data of reference [5] were obtained using a 5s drop tower which may be relied upon as steady state spread rate data. It is also interesting to note that the spread rate reaches steady state value (within 5%) at about 3s. At this time the flame shape at the trailing tip is still developing. This is because the flame spread rate is primarily driven by the leading edge of the flame and trailing part has little effect on spread rate.

The variation of flame spread rate and variation of integrated heat flux over the preheated region with time are shown in figure 3 and figure 4. While transient flame spread can be seen as an indicator of time response of solid phase (as flame spreads on account of fuel pyrolysis), the transient integrated heat flux over the preheat zone can be considered as an indicator of gas phase time response (heat feedback to thin fuel is primarily from gas phase directly). It should be noted that at steady state flame

spread rate is directly proportional to the integrated heat flux on the solid fuel over the preheat region (*i.e.* higher spread rate means higher integrated heat flux) but in transient situations as the gas phase and solid phase may respond at different rates. A close observation of fig. 3 & fig. 4 show that instantaneous spread rate and the integrated net heat flux in the preheat region are not in phase. This difference in phase leads to non-monotonic (or oscillatory) transient response in the spread rate. In the complex reactive flow field coupled with heat and mass transport the following phenomenological explanation may be given for the oscillation. The solid fuel responds by releasing more fuel vapor to an increase in heat flux from gas phase but because the response is slower compared to gas phase, during the period the gas heat flux already begin to drop. Now the presence of excess fuel vapor increases flame size and heat flux feed back to the solid again while solid is responding to reduced heat flux. In this way out of phase heat feedback and solid response may lead to oscillation.

3.2 Flame spread transition from $0g$ to $1g$

Sudden transition from $0g$ to higher gravity levels is encountered at the end of tests in microgravity tower and at the pull up phase of parabolic flight. These gravity levels are usually several times higher than normal gravity level. Here for comparison with the above study we consider sudden switch from $0g$ to $1g$ gravity environment. All other conditions are kept same as in the case discussed in the previous section.

The microgravity flame (close to one shown in fig. 5 at $t = 0.001s$) is long with trailing edge reaching about 30cm downstream of flame anchor point and located above 2cm from fuel surface. Sudden exposure to normal gravity field induces upward buoyant acceleration in hot combustion products and an inward (along negative Y direction) flow from ambient to replace rising mass. This pushes the flame close to the surface while convecting it downstream. The long trailing edge of flame gets trimmed of to a short length flame. The difference in response time of solid and gas phase (0.024s and 0.004s respectively) results in oscillatory flame spread transient (fig. 6). Since the time scales in normal gravity environment are much smaller (owing to large convective flow field) compared to zero-gravity environment, the oscillation frequency is higher and the final steady state for normal gravity is reached in a much shorter time period of about 1.1s.

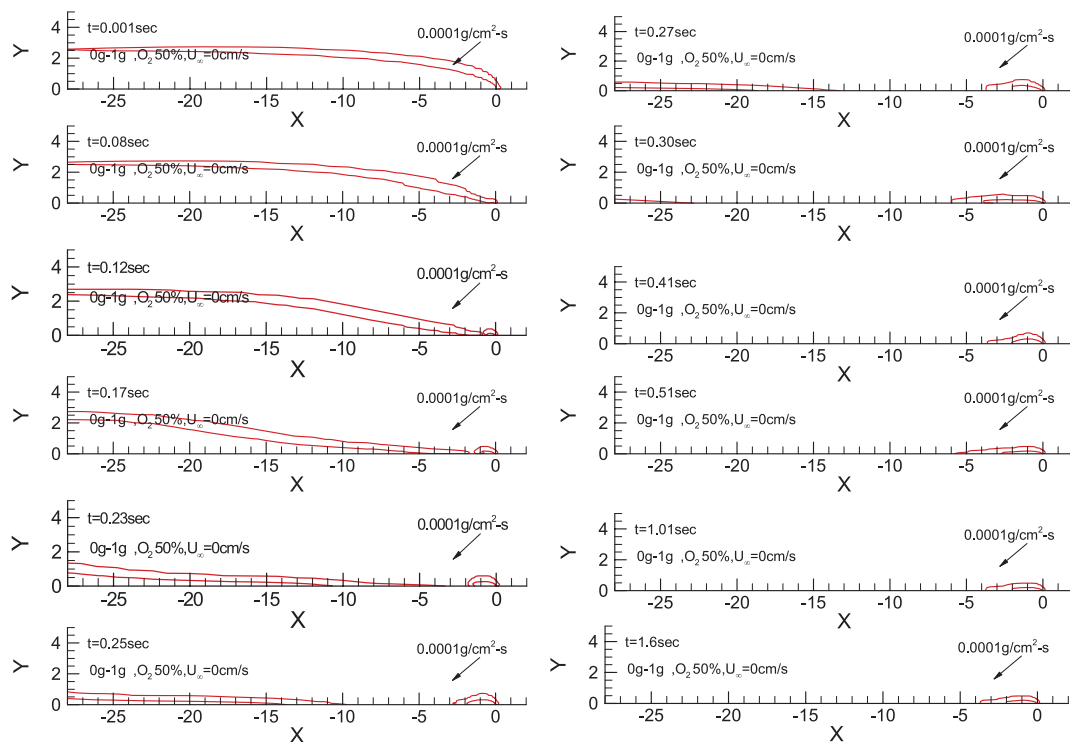


Figure 5. Flame shape (represented by reaction rate contour) at different instances of times for sudden transition from $0g$ to $1g$

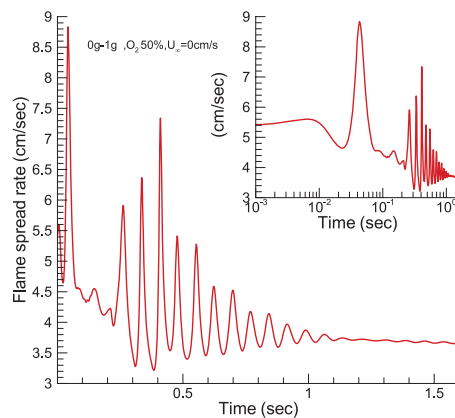


Figure 6. Flame spread rate variation with time for sudden transition from $0g$ to $1g$ environment

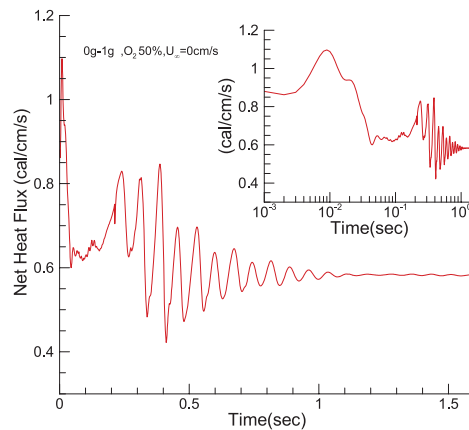


Figure 7. Time Variation of integrated heat flux along preheated region of the solid fuel for sudden transition from $0g$ to $1g$ environment

A closer look at flame spread transient (fig. 6) and the time variation of the integrated heat flux over the preheated region of the solid fuel (fig. 7) shows that the integrated heat flux is almost out of phase with the flame spread rate. For example when flame spread rate peaks at about 0.35s the integrated heat flux has dropped to the minimum.

CONCLUSION

A numerical study was carried out to study the opposed flow flame spread transient for sudden transition from normal gravity ($1g$) to zero-gravity ($0g$) and vice versa. The following conclusions can be drawn from this study.

1. The time required for flame spread rate to reach steady state in a normal gravity ($1g$) to zero-gravity ($0g$) transition could be of the order of few seconds (here about 3-4s). Hence such microgravity experimental studies should be conducted in facilities with available testing time of the order of 5s or more. A short duration (2s or less) test may not give steady state data. In comparison the time required to reach steady state spread in a zero-gravity ($0g$) to normal-gravity ($1g$) (or higher gravities as may be the case in real scenario) transition is of the order of a fraction of second (here about 1s).
2. The flame spread rate transient in both $1g-0g$ and $0g-1g$ sudden transition was oscillatory. This oscillatory nature is due to different response time of the gas phase and the solid phase which results in phase lag between processes of heat feedback from gas to solid fuel and fuel heating-up and pyrolysis. It should be noted that in steady spread the flame spread rate is directly proportional to heat feedback to the solid fuel.

ACKNOWLEDGEMENT

Authors would like to thank the reviewers of ICEAE 2009 for scrutinizingly going through the paper and for their valuable suggestions which has greatly enhanced the quality of this work.

REFERENCES

- [1] Di Blasi, C. "Ignition and Flame Spread Across Solid Fuels," *Prog. Astro. Aero.* **35**, Oran and Boris (Eds.) (1991) 643-671.
- [2] Mell, W. E.; and Kashiwagi, T. "Dimensional Effects on the Transition from Ignition to Flame Spread in Microgravity," *Proc. Combust. Inst.*, **27** (1998) 2635-2641.
- [3] Kazuyoshi Nakabe, Howard R. Baum, and Takashi Knshiwagi, "Ignition And Subsequent Flame Spread Over a Thin Cellulosic Material", *2nd International Microgravity Combustion Workshop*, 167-179 pp, 1992
- [4] Robert A. Altenkirch, Lin tang, Kurt Sacksteder, Subrata Bhattacharjee and Michael A Delichatsios, "Inherently Unsteady Flame Spread To Extinction Over Thick Fuels in Microgravity", Twenty-Seventh Symposium (International) on Combustion/The Combustion Institute, pp. 2515–2524, 1998.
- [5] Takahashi Shuhei, Wakai Kazunori, Paolini Chris and Bhattacharjee Subrata, "Transition between Concurrent and Opposed Flow Flame Spread over Thin Films of PMMA in a Microgravity Environment", *Proceedings of Thermal Engineering Conference* (2005).
- [6] Ferkul.P.V, A Model of Concurrent Flow Flame Spread Over Thin Solid Fuel, *Ph.D.Dissertation, Case Western Reserve University, Cleveland, OH*, (1993).
- [7] Jiang.C.B, A Model of Flame Spread over a Thin Solid in Concurrent Flow with Flame Radiation, *Ph.D.Dissertation, Case Western Reserve University, Cleveland, Oh* (1995).
- [8] Shih.H.Y and T'ien.J.S, Modelling Concurrent Flame spread Over a thin Solid in Low-Speed Flow Tunnel, *Proc.Combust.Inst.*, **28**, (2000), 2777.
- [9] Smooke.M.D and Giovangigli.V, Formulation of the Premixed and Nonpremixed Test Problem, *lecture Notes in Physics, Series 384, Chapter 1*, Spring-Verlag, Newyork, 1991.
- [10] Hoffman .Z, *Gas Dynamics*, John Wiley& Sons Inc., New York, 1976.
- [11] Lefebvre.A.H, *Gas Turbine Combustion*, McGraw Hill Inc., New York, 1983.
- [12] Grayson.G, Sacksteder.,K.R, Ferkul.P.V.and T'ien. James. S, *Microgravity sci. Tech.* **7**(2) (1994) 187-193.
- [13] Di Blasi.C, Prediction of Wind-opposed Flame Spread Rates and Energy Feedback Analysis for Charring Solids in a Microgravity Environment, *Combust. Flame*, **100**:332-340(1995).
- [14] Bhattacharjee.S and Altenkirch.R.A, Radiation Controlled, Opposed-Flow Flame Spread in a Microgravity Environment, *Proc. Combust. Inst.*, **23**, (1990b), 1627-1633.
- [15] Lin.Tzung-hsien and Chen. Chiun-Hsun, "Influence of Two-dimensional Gas Phase Radiation on Downward Flame Spread", *Combust.Sci. and Tech.*, **141**(1999)83-106.
- [16] Rhatigan. J, Bedir.H and T'ien,J.S, Gas Phase Radiative Effects on the Burning and Extinction of a Solid, *Combust.Flame* , **112**, (1998), 231-241.
- [17] Pettegrew, R., Street, K., Plitch, N., T'ien, J. S. and Morrison, P., "Measurement and Evaluation of the radiative Properties of Thin Solid Fuels," AIAA paper no 2003-0511, 2003.
- [18] Patankar. S. V, *Numerical Heat Transfer and Fluid Flow* (New York: Hemisphere) 1980
- [19] Sandra. L.Olson, The Effect of Microgravity on Flame spread Over a Thin fuel, *M. S. Dissertation, Case Western Reserve University, Cleveland, OH*, (1987).

